The sensitivity characteristics of tilted fibre Bragg grating sensors with different cladding thicknesses

2007 Meas. Sci. Technol. 18 3117

(http://iopscience.iop.org/0957-0233/18/10/S11)

Meas. Sci. Technol. **18** (2007) 3117–3122 doi:10.1088/0957-0233/18/10/S11

The sensitivity characteristics of tilted fibre Bragg grating sensors with different cladding thicknesses

C Chen[1], C Caucheteur[2], P Mégret[2] and J Albert[1]

[1] Department of Electronics, Carleton University, 1125 Colonel By Drive, Ottawa, K1S 5B6, Canada
[2] Faculté Polytechnique de Mons, Service d'Electromagnétisme et de Télécommunications, Boulevard Dolez 31, 7000 Mons, Belgium

E-mail: jalbert@doe.carleton.ca

Received 31 December 2006, in final form 21 February 2007
Published 12 September 2007
Online at stacks.iop.org/MST/18/3117

Abstract
In this paper, we present the sensitivity characteristics of core and cladding modes in weakly tilted fibre Bragg grating sensors with different cladding thicknesses. Both experimental and analysis results are presented. The results show that the strain sensitivity of cladding mode resonances in tilted fibre Bragg gratings does not depend on the cladding diameter but on the wavelength separation from the core resonance over the range of the cladding diameters studied.

Keywords: Fibre sensors, fibre Bragg gratings, strain, sensitivity

(Some figures in this article are in colour only in the electronic version)

1. Introduction

Tilted fibre Bragg grating (TFBG) sensors [1–8] have attracted attention recently because a single TFBG can perform as a temperature-independent strain sensor [1, 3, 8], a temperature-independent external refractive index sensor [2–4, 7] and a bend sensor [5]. Otherwise, these functions require the use of two fibre Bragg gratings (FBG) [9], hybrid FBG with long period gratings (LPG) [10], superimposed FBGs [11] and high birefringence fibre gratings [12].

In the TFBG, both a core mode resonance and several cladding mode resonances appear simultaneously in the transmission spectrum. This has several advantages. The cladding mode resonances are sensitive to the external perturbations (refractive index, deposited layer thicknesses, etc), while the core mode (Bragg) resonance is only sensitive to axial strain and temperature. It has been observed that the temperature dependence of cladding modes is similar to that of the core modes, so that the effect of temperature can be removed from the cladding mode resonance by monitoring the wavelength difference between the core mode resonance and selected cladding mode resonances [3]. Using this technique, temperature-independent strain and external refractive index sensors can be made.

In order to enhance the external refractive index sensitivity of both FBG and LPG, thinned cladding layer thicknesses are preferred [13, 14]. In the case of TFBGs, the effect of reducing the cladding layer thickness for an external refractive index sensor is shown to increase the sensitivity substantially [3, 4]. In the work presented here, we report both experimental and analytical results on the differential strain and temperature sensitivities of cladding and core mode resonances in fibres with reduced cladding diameter. The fibres studied are a standard Corning SMF-28 fibre etched to reduce its outer diameter to 50 μm, and a specially fabricated 50 μm cladding layer diameter experimental fibre (also from Corning, and otherwise similar to SMF-28).

2. Analysis

As is well known, the Bragg reflection and cladding mode resonance wavelengths λ_B and λ^i_{clad} of TFBG are determined by a phase-matching condition and can be expressed as follows [3]:

$$\lambda_B = 2n_{\text{eff}}\Lambda/\cos\theta \tag{1}$$

$$\lambda^i_{\text{clad}} = \left(n^i_{\text{eff,core}} + n^i_{\text{eff,clad}}\right)\Lambda\big/\cos\theta \tag{2}$$

where n_{eff}, $n^i_{\text{eff,core}}$ and $n^i_{\text{eff,clad}}$ are the effective indices of the core mode at λ_B and the core mode and the ith cladding mode at λ^i_{clad} respectively, and Λ and θ are the period and the internal tilt angle of the TFBG. For weakly TFBG, if we consider the Bragg and cladding mode wavelength shifts $\left(\Delta\lambda_B, \Delta\lambda^i_{\text{clad}}\right)$ caused by axial strain $(\Delta\varepsilon)$ and temperature changes (ΔT), from equations (1) and (2) the wavelength shifts $\Delta\lambda_B$ and $\Delta\lambda^i_{\text{clad}}$ can be written as follows:

$$\Delta\lambda_B = \left(\frac{2n_{\text{eff}}}{\cos\theta}\frac{\partial\Lambda}{\partial\varepsilon} + \frac{2\Lambda}{\cos\theta}\frac{\partial n_{\text{eff}}}{\partial\varepsilon}\right)\Delta\varepsilon + \left(2\frac{\Lambda}{\cos\theta}\frac{\partial n_{\text{eff}}}{\partial T} + 2\frac{n_{\text{eff}}}{\cos\theta}\frac{\partial\Lambda}{\partial T}\right)\Delta T \tag{3}$$

$$\Delta\lambda^i_{\text{clad}} = \left(\frac{\left(n^i_{\text{eff,core}} + n^i_{\text{eff,clad}}\right)}{\cos\theta}\frac{\partial\Lambda}{\partial\varepsilon} + \frac{\Lambda}{\cos\theta}\frac{\partial\left(n^i_{\text{eff,core}} + n^i_{\text{eff,clad}}\right)}{\partial\varepsilon}\right)\Delta\varepsilon + \left(\frac{\Lambda}{\cos\theta}\frac{\partial\left(n^i_{\text{eff,core}} + n^i_{\text{eff,clad}}\right)}{\partial T} + \frac{n^i_{\text{eff,core}} + n^i_{\text{eff,clad}}}{\cos\theta}\frac{\partial\Lambda}{\partial T}\right)\Delta T. \tag{4}$$

If we only consider the wavelength shifts $\Delta\lambda_B$ and $\Delta\lambda^i_{\text{clad}}$ caused by axial strain changes $(\Delta\varepsilon)$, equations (3) and (4) can be written as follows [15]:

$$\Delta\lambda_B = \lambda_B\left(1 - p_B\right)\Delta\varepsilon \tag{5}$$

$$\Delta\lambda^i_{\text{clad}} = \lambda^i_{\text{clad}}\left(1 - p^i_{\text{cld}}\right)\Delta\varepsilon \tag{6}$$

where

$$p_B = -\frac{1}{n_{\text{eff}}}\frac{\partial n_{\text{eff}}}{\partial\varepsilon} \tag{7}$$

and

$$p^i_{\text{clad}} = -\frac{1}{n^i_{\text{eff,core}} + n^i_{\text{eff,clad}}}\frac{\partial\left(n^i_{\text{eff,core}} + n^i_{\text{eff,clad}}\right)}{\partial\varepsilon} \tag{8}$$

are photoelastic coefficients for core (Bragg) mode and the ith cladding modes respectively, which may be calculated through core and cladding refractive index changes by

$$\delta n = 0.5 * n^3\left[p_{12} - \nu(p_{11} - p_{12})\right]\delta\varepsilon \tag{9}$$

where p_{11} and p_{12} represent the component of strain-optic tensor, ν is Poisson's ratio and n is the core or cladding refractive index. The high order cladding modes have smaller effective indices and hence will have larger photoelastic coefficients than the core mode if the partial derivatives of all the effective indices with respect to a global strain change on the fibre are similar. From equations (5) and (6) and noting that $\lambda_B > \lambda^i_{\text{clad}}$ and $p_B < p^i_{\text{clad}}$ for high order cladding modes, we obtain

$$\Delta\lambda_B = \lambda_B(1 - p_B)\Delta\varepsilon > \lambda^i_{\text{clad}}(1 - p_B)\Delta\varepsilon > \lambda^i_{\text{clad}}\left(1 - p^i_{\text{clad}}\right)\Delta\varepsilon = \Delta\lambda^i_{\text{clad}}. \tag{10}$$

So the Bragg peak should have a larger wavelength shift than the high order cladding mode resonances.

3. Experimental results

The experimental TFBG sensors are written in hydrogen-loaded Corning SMF-28 fibres and Corning thin cladding layer experimental fibre by a 248 nm KrF excimer laser light and a phase mask to generate the grating pattern. The Bragg and cladding mode resonance wavelengths are determined by the grating period of the phase mask used and the effective indices of each mode. In our experimental set-up, when the tilt angle θ changes, the projection of the grating period along the fibre axis does not change (since both the fibre and mask are rotated together in the plane of incidence of the laser beam). Therefore changing the tilt angle changes the cladding mode resonance envelope (i.e. the strength of the couplings) but not the resonance wavelength positions. Figure 1 shows transmission spectra of three TFBG sensors: figure 1(*a*) the TFBG is written in a SMF-28 fibre with tilt angle $\theta = 4^\circ$, figure 1(*b*) the TFBG is written in a Corning experimental 50 μm cladding layer diameter fibre with tilt angle $\theta = 6^\circ$ and figure 1(*c*) the TFBG is first written in a SMF-28 fibre with tilt angle $\theta = 4^\circ$, then etched in 50% HF (water solution) to 50 μm cladding layer diameter. It can be seen from figure 1 that the thinner cladding layer thickness results in fewer cladding modes that are more widely separated in wavelength. This provides the added benefit that it becomes much easier to track individual resonances. One remarkable feature is that while cases figures 1(*b*) and (*c*) are nominally equivalent (apart from the tilt angle), the spectral quality of grating figure 1(*c*) is much poorer (broader, poorly defined resonances, especially at shorter wavelengths). It is suspected that the poor spectral quality is caused by surface roughness remaining after the etching process, while the fibre of figure 1(*b*) has the pristine surface of pulled fibre.

An important feature of the two low tilt angle results figures 1(*a*) and (*c*) is the presence of a strong 'ghost mode' resonance, immediately to the left of the Bragg (core mode) resonance. This ghost mode is made up of several low order fibre modes and is known to be very sensitive to bending [5], but very little to outside refractive index [3].

Figure 2 shows the relative wavelength shifts of cladding resonances with respect to the Bragg resonance when longitudinal strain and temperature perturbations are applied to a TFBG in standard SMF-28 fibre with $d = 125$ μm and $\theta = 4^\circ$. It can be seen for the strain perturbation that there are three differential wavelength shift regions. First, within 5 nm from the Bragg resonance, the ghost mode appears to be very sensitive to external strain perturbations and there are even some low order cladding mode resonances that appear to have negative relative wavelength shifts (in contrast to the theory presented in section 2). We believe that the apparent negative shift is an artefact due to our inability to distinguish several closely separated resonances that change amplitude when strain is applied. This occurs in such a way that modes closer to the Bragg peak increase their coupling strength and our peak search algorithm jumps modes in this wavelength region (hence simulating a relative shift of the resonance towards the Bragg peak). For higher order modes, further than 20 nm from the Bragg resonance, the results are quite irregular and there are several cladding modes with double peaked resonances which appear to have very large relative

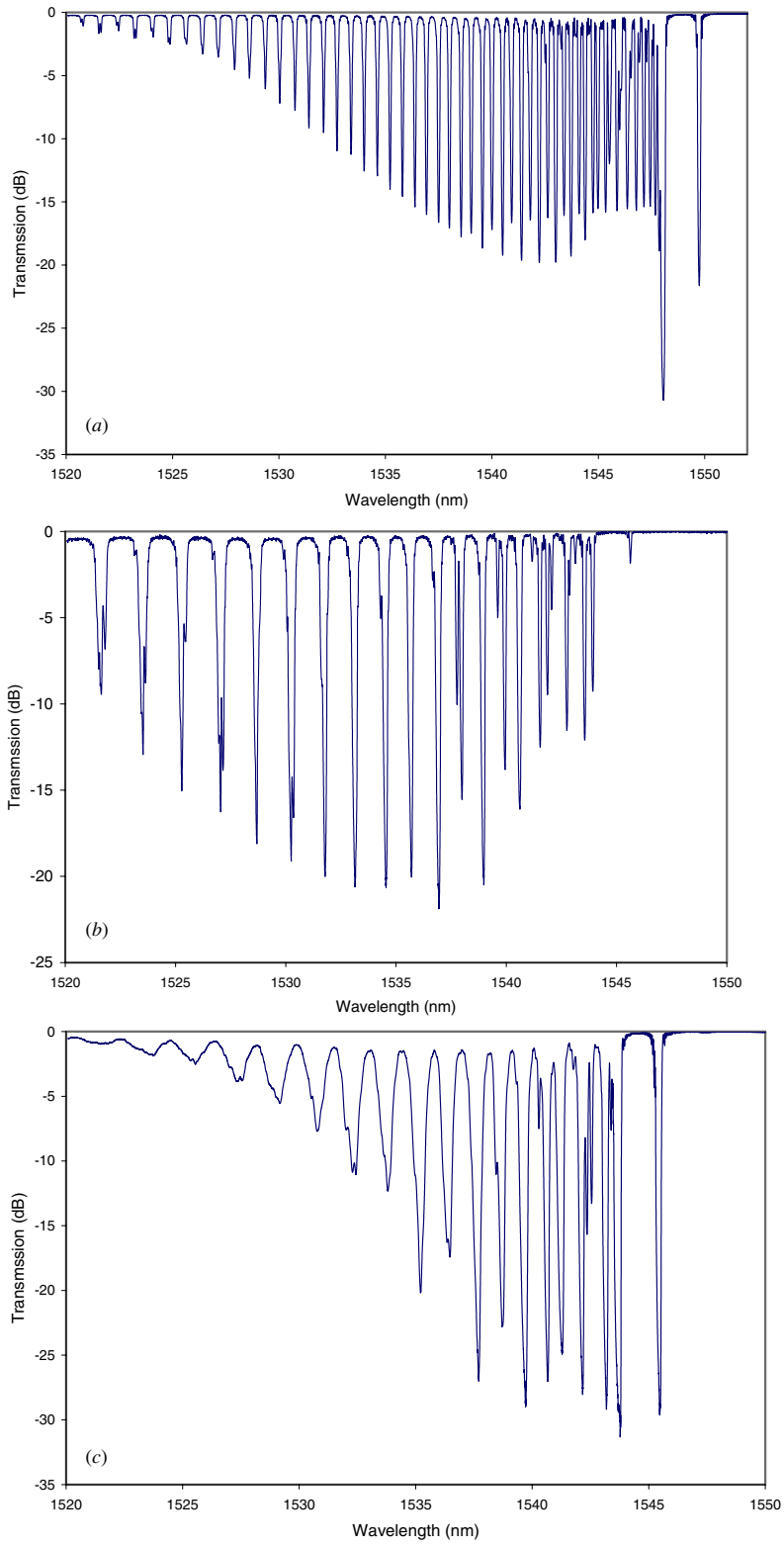

Figure 1. The transmission spectra of weakly TFBG: (*a*) SMF-28 fibre $d = 125$ μm and $\theta = 4^\circ$; (*b*) Corning experimental thin cladding layer fibre $d = 50$ μm and $\theta = 6^\circ$; (*c*) thin cladding layer by HF etching from SMF-28 fibre $d = 50$ μm and $\theta = 4^\circ$.

wavelength shifts. Again, these irregular shifts may be due to improper peak tracking within the double peaks rather than to actual strain sensitivity. Finally, between 5 nm and 20 nm from the Bragg resonance there is a wavelength region where the differential wavelength shift grows very linearly with mode order and with strain. The lower part of the graph shows that the relative wavelength shifts of cladding resonances to the Bragg resonance with temperature from -9.7° to 59.5° is very

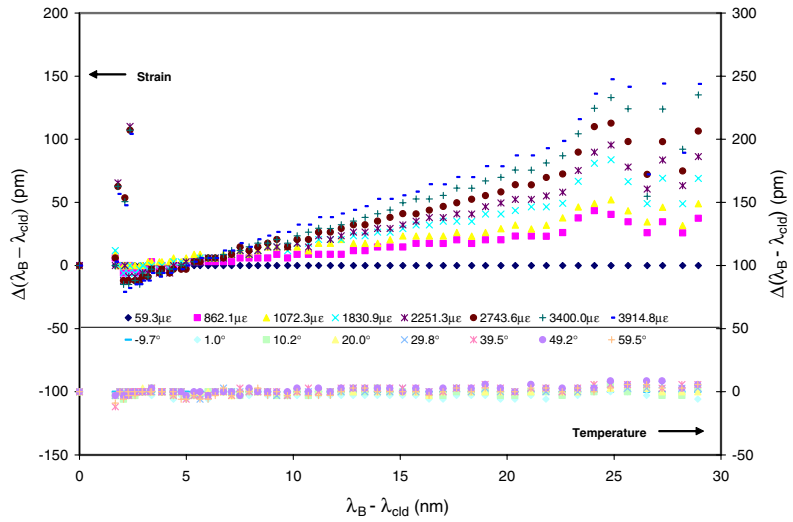

Figure 2. The relative wavelength shift of cladding mode resonances to the Bragg resonance of TFBG with standard SMF-28 fibre $d = 125$ μm and $\theta = 4^\circ$ due to longitudinal strain and temperature perturbations.

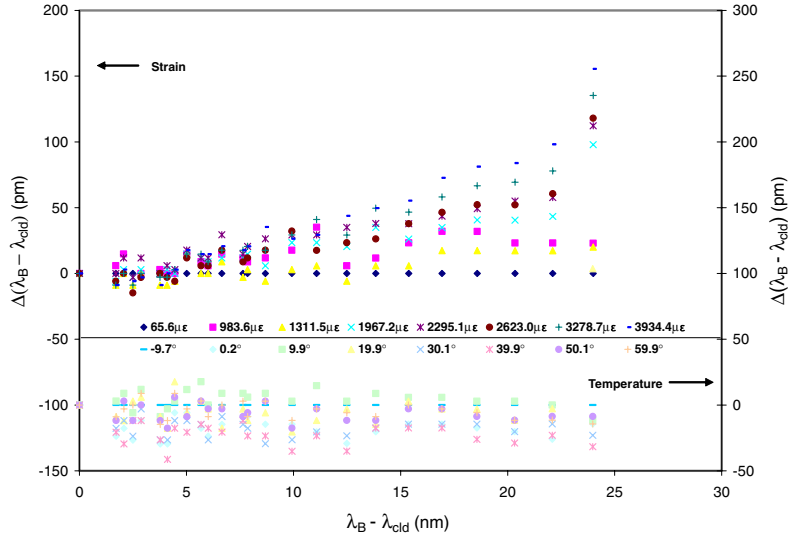

Figure 3. The relative wavelength shift of cladding mode resonances to the Bragg resonance of TFBG with thin cladding layer $d = 50$ μm and $\theta = 6^\circ$ due to longitudinal strain and temperature perturbations.

small; it is around ± 12 pm corresponding to 0.35 pm $^\circ C^{-1}$ if it was linear.

Figure 3 shows exactly the same measurements for the experimental fibre with 50 μm cladding diameter and $\theta = 6^\circ$. While the appearance of the graph is similar to figure 2, there are notable differences. Most importantly, the resonance shift behaviour with increasing strain is much less regular, especially for low strain values and the maximum variations due to temperature changes between -9.7° and 59.5° are about two times larger (between -41 and $+17$ pm or 0.8 pm $^\circ C^{-1}$). It appears as if the linear regular region of 'well behaved' modes observed between -5 and -20 nm from the Bragg resonance in standard fibre has been squeezed away in the reduced cladding fibre, leaving only complex resonances made up of multiple vector modes [16] in the low mode order region and for modes nearing cut-off.

A direct comparison of the two types of fibres for a high strain value in each case (3855 $\mu\varepsilon$ and 3868 $\mu\varepsilon$) is provided in figure 4. Apart from irregular regions at both ends of the mode spectra in each case, the differential strain is equal for the two fibres when considering resonances that are located at the same distance from the Bragg peak. It is clear from this graph that the dominant feature of the differential strain sensitivity is the wavelength spacing between the resonances (or equivalently the difference in the effective index of the cladding mode in question to that of the core mode), even though the mode order (and hence its cross sectional shape across the cladding) is quite different for fibres that are so different in size. It is worth mentioning that the tilt angle was not even the same for these two results, further highlighting the insensitivity of the differential wavelength shift technique to the exact value of tilt angle. Finally, much of the irregular behaviour observed

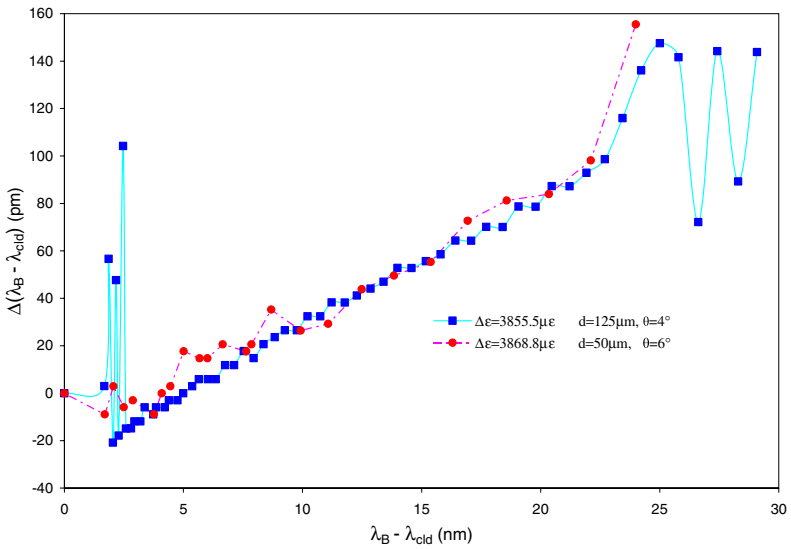

Figure 4. Differential wavelength shift of individual resonances for thin and regular fibres near 3860 $\mu\varepsilon$.

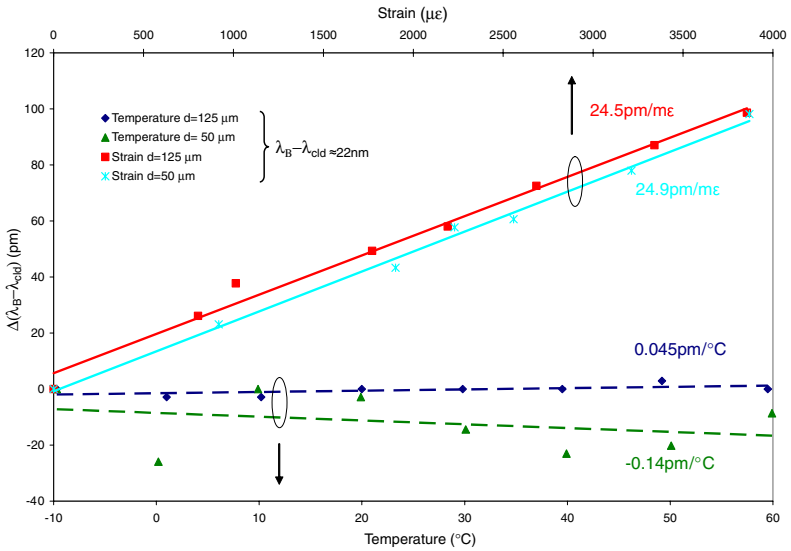

Figure 5. Comparison of differential wavelength shifts of cladding mode resonances for a 4° tilted FBG in SMF-28 fibre and a 6° tilted FBG in Corning experimental 50 μm diameter thin cladding fibre ∼22 nm away from their Bragg resonances due to strain and temperature perturbations.

for low and for high order modes could be resolved by a more accurate individual mode resonance position determination for these quasi-degenerate resonances made up of several vector modes.

Figure 5 shows two single cladding resonance wavelength shifts due to strain and temperature perturbations at resonance peaks about 22 nm away from their Bragg resonances in two different diameter fibres: one is 125 μm cladding layer diameter SMF-28 fibre and the other is 50 μm cladding layer diameter Corning experimental fibre. From the results, we can see that the differential wavelength shifts of the two TFBGs increase almost linearly as the strain increases. The strain sensitivities of the differential wavelength shifts are 24.5 pm mε^{-1} for TFBG in SMF-28 fibre and 24.9 pm mε^{-1} for TFBG in thin cladding layer fibre and the differential wavelength shifts due to the temperature changes are 0.045 pm $^{\circ}$C^{-1} and -0.14 pm $^{\circ}$C^{-1}, respectively. If we interrogate these two resonances without independent knowledge of temperature, the error due to temperature fluctuations corresponds to an uncertainty of ± 129 $\mu\varepsilon$ for cladding resonance of TFBG in SMF-28 fibre and ± 394 $\mu\varepsilon$ for cladding resonance of TFBG in thin cladding layer fibre.

4. Conclusions

In summary, the strain and temperature sensitivities of weakly TFBG with different cladding thicknesses have been presented and tested experimentally. A thin cladding layer thickness results in fewer cladding modes that are more widely separated in wavelength; therefore it increases the range of external perturbation measurements achievable with a single resonance without facing an uncertainty about which resonance is observed. Unlike grating-based refractive index sensors, in which a thin cladding layer thickness is preferred for

high sensitivity of the cladding mode resonance to external refractive changes, a thin cladding layer thickness does not change the strain sensitivity of cladding mode resonances, but it slightly increases the relative temperature dependence of cladding mode wavelength shift to Bragg wavelength shift from 0.35 pm $^{\circ}C^{-1}$ to 0.8 pm $^{\circ}C^{-1}$ (between 125 μm and 50 μm diameter fibres). We have clearly shown that the strain sensitivity of individual cladding resonances is uniquely determined by the wavelength separation between the resonance and the Bragg resonance, irrespective of cladding diameter. In addition, we showed that achieving thin cladding thicknesses by HF etching of standard fibres reduces the spectral quality of individual transmission resonances especially for high order modes with larger amplitudes at the etched surface (however, for envelope-based interrogation schemes this does not pose a problem [4], and the fibres that are thinned only near the gratings are much easier to splice to conventional fibres).

Acknowledgment

This project is supported by LxSix Photonics, the OGSST (C Chen) and the Fonds National de la Recherche Scientifique (C Caucheteur). J Albert holds the Canada Research Chair in Advanced Photonic Components.

References

[1] Kang S C, Kim S Y, Lee S B, Kwon S W, Choi S S and Lee B 1998 Temperature-independent strain sensor system using a tilted fiber Bragg grating demodulator *IEEE Photon. Technol. Lett.* **10** 1461–3

[2] Laffont G and Ferdinand P 2001 Tilted short-period fibre-Bragg-grating-induced coupling to cladding modes for accurate refractometer *Meas. Sci. Technol.* **12** 765–70

[3] Chen C, Xiong L, Jafari A and Albert J 2005 Differential sensitivity characteristics of tilted fiber Bragg grating sensors *Proc. SPIE.* **6004** 6004–13

[4] Caucheteur C, Chah K, Lhommé F, Debliquy M, Lahem D, Blondel M and Mégret P 2005 Enhancement of cladding modes couplings in tilted Bragg gratings owing to cladding etching *Workshop on Fibres and Optical Passive Components (WFOPC)* p 234

[5] Baek S, Jeong Y and Lee B 2002 Characteristics of short-period blazed fiber Bragg gratings for use as macro-bending sensors *Appl. Opt.* **41** 631–6

[6] Chen C and Albert J 2006 Strain-optic coefficients of individual cladding modes of singlemode fibre: theory and experiment *Electron. Lett.* **42** 1027–8

[7] Chan C F, Chen C, Jafari A, Laronche A, Thomson D J and Albert J 2007 Optical fiber refractometer using narrowband cladding mode resonance shifts *Appl. Opt.* **46** 1142–9

[8] Chen X, Zhou K, Zhang L and Bennion I 2006 In-fiber twist sensor based on a fiber Bragg grating with 81 degrees tilted structure *IEEE Photon. Technol. Lett.* **18** 2596–8

[9] Shu X, Lin Y, Zhao D, Gwandu B, Floreani F, Zhang L and Bennion I 2002 Dependence of temperature and strain coefficients on fiber grating type and its application to simultaneous temperature and strain measurement *Opt. Lett.* **27** 701–3

[10] Chen X, Zhou K, Zhang L and Bennion I 2005 Simultaneous measurement of temperature and external refractive index by use of a hybrid grating in D fiber with enhanced sensitivity by HF etching *Appl. Opt.* **44** 178–82

[11] Xu M G, Archambault J L, Reekie L and Dakin J P 1994 Discrimination between strain and temperature effects using dual wavelength fibre sensors *Electron. Lett.* **30** 1085–7

[12] Chen G H, Liu L Y, Jia H Z, Yu J M, Xu L and Wang W C 2003 Simultaneous pressure and temperature measurement using Hi-Bi fiber Bragg gratings *Opt. Commun* **228** 99–105

[13] Iadicicco A, Cusano A, Cutolo A, Berini R and Giordano M 2004 Thinned fiber Bragg gratings as high sensitivity refractive index sensor *IEEE Photon. Technol. Lett.* **16** 1149–51

[14] Chung K W and Yin S 2004 Analysis of a widely tunable long-period grating by use of an ultrathin cladding layer and higher-order cladding mode coupling *Opt. Lett.* **29** 812–4

[15] Othonos A and Kalli K 1999 *Fiber Bragg Gratings* (Boston, MA: Artech House)

[16] Lee K S and Erdogan T 2000 Fiber mode coupling in transmissive and reflective tilted fiber gratings *Appl. Opt.* **39** 1394–404